ELSEVIER

Biochimica et Biophysica Acta 1323 (1997) 240–252

BIOCHIMICA ET BIOPHYSICA ACTA
BBA

Dielectrophoretic detection of changes in erythrocyte membranes following malarial infection

Peter Gascoyne [a,*], Ronald Pethig [b], Jutamaad Satayavivad [c], Frederick F. Becker [a], Mathuros Ruchirawat [c]

[a] *Section of Experimental Pathology, Box 89, University of Texas M.D. Anderson Cancer Center, 1515 Holcombe Boulevard, Houston, TX 77030, USA*

[b] *Institute of Molecular and Biomolecular Electronics, University of Wales, Dean Street,Bangor, Gwynedd LL57 1UT, UK*

[c] *Chulabhorn Research Institute, Lak Si, Vipavadee-Rangsit Highway, Bangkok 10210, Thailand*

Received 3 April 1996; revised 1 August 1996; accepted 10 September 1996

Abstract

The dielectric properties of normal erythrocytes were compared to those of cells infected with the malarial parasite *Plasmodium falciparum*. Normal cells provided stable electrorotation spectra which, when analyzed by a single-shelled oblate spheroid dielectric model, gave a specific capacitance value of 12 ± 1.2 mF/m^2 for the plasma membrane, a cytoplasmic permittivity of 57 ± 5.4 and a cytoplasmic conductivity of 0.52 ± 0.05 S/m. By contrast, parasitized cells exhibited electrorotation spectra with a time-dependency that suggested significant net ion outflux via the plasma membrane and it was not possible to derive reliable cell parameter values in this case. To overcome this problem, cell membrane dielectric properties were instead determined from dielectrophoretic crossover frequency measurements made as a function of the cell suspending medium conductivity. The crossover frequency for normal cells depended linearly on the suspension conductivity above 20 mS/m and analysis according to the single-shelled oblate spheroid dielectric model yielded values of 11.8 mF/m^2 and 271 S/m^2, respectively, for the specific capacitance and conductance of the plasma membrane. Unexpectedly, the crossover frequency characteristics of parasitized cells at high suspending medium conductivities were non-linear. This effect was analyzed in terms of possible dependencies of the cell membrane capacitance, conductance or shape on the suspension medium conductivity, and we concluded that variations in the membrane conductance were most likely responsible for the observed non-linearity. According to this model, parasitized cells had a specific membrane capacitance of 9 ± 2 mF/m^2 and a specific membrane conductance of 1130 S/m^2 that increased with increasing cell suspending medium conductivity. Such conductivity changes in parasitized cells are discussed in terms of previously observed parasite-associated membrane pores. Finally, we conclude that the large differences between the dielectrophoretic crossover characteristics of normal and parasitized cells should allow straightforward sorting of these cell types by dielectrophoretic methods.

Keywords: Malaria; Erythrocyte; Dielectric; Membrane conductivity; Membrane capacitance; (*Plasmodium falciparum*)

1. Introduction

It is well established that erythrocytes that have become infected with malarial merozoites experience a number of fundamental changes to their plasma

Abbreviations: DEP, dielectrophoresis; ROT, electrorotation

* Corresponding author. Fax: +1 (713) 7925940; e-mail: peter@solace.mda.uth.tmc.edu.

PII S0005-2736(96)00191-5

membrane properties as the parasites develop inside [1–3]. Morphologically, electron microscopic investigations have revealed electron-dense knobs protruding from the plasma membrane surface of infected cells and caveola–vesicle complexes along their borders [4–6]. On the molecular scale, parasitization results in significant changes in the membrane phospholipid composition [7–10], some normal surface proteins are suppressed [11] while new proteins are expressed [4,12,13], and the composition of the glycocalyx is altered [14,15]. A number of modifications to the biophysical properties of the erythrocyte membrane also occur, including a decrease in its net negative charge [16] and an increase in rigidity [17], factors that may play a role in the adherence of infected cells to capillary beds in the target organs of malaria patients. Despite the enhanced overall rigidity, the local fluidity of membrane lipids is increased [7,18,19], and membrane permeability to water and to a variety of ionic and neutral substances rises sharply to meet the increasing demand for essential nutrients and for the elimination of waste metabolites of the developing parasite [3,20–23].

Not surprisingly, such extensive changes in the composition, morphology and permeability of the erythrocyte membrane produce corresponding alterations in the electrical and dielectric properties of infected cells. Thus, Aceti et al. [24] reported that *Plasmodium falciparum*-infected human erythrocytes exhibit an increased plasma membrane electrical conductivity in the frequency range 10 kHz–100 MHz when examined in bulk suspension. The interpretation of such bulk suspension measurements in terms of the underlying cell biological changes, particularly for mixtures of cells in different stages of parasitemia, is difficult, however. We and others have demonstrated that the AC electrokinetic techniques of electrorotation (ROT) and dielectrophoresis (DEP) permit non-invasive dielectric measurements to be made on individual cells [25–28], revealing the plasma membrane capacitance and conductance as well as morphological data with single cell discrimination [29,30]. Such measurements permit the true dielectric dispersion widths to be derived and their subcellular origins to be probed without the confounding effects of population distributions that are inherent in bulk measurements. Furthermore, single cell measurements provide the opportunity for the dielectric characterization of different cell types within a cell mixture and the dielectric properties derived for each type can then be exploited for selectively manipulating target cell subpopulations using AC electrokinetics. Using this approach, we recently demonstrated that leukemia [31] and metastatic breast cancer [32] cells could be separated from human blood using dielectrophoretic principles on the basis of such differential electrical characteristics and others have applied these principles to the separation of non-viable from viable yeast cells [33], and to the enrichment of human hemopoietic (CD34 +) cells [34].

The possibility of characterizing individual malarial cells, selectively manipulating them in mixtures with normal cells, and separating them has obvious research and diagnostic implications. Therefore, we have applied AC electrokinetic methods to investigate the dielectric properties of human erythrocytes infected with *P. falciparum* to test the feasibility of dielectrophoretic methods for discriminating between parasitized and healthy cells. We show here that *P. falciparum*-infected red cells exhibit a non-linear DEP crossover frequency response to increasing cell suspension conductivity. We discuss this response in terms of changes in cell membrane conductance, capacitance and shape. We conclude that the most plausible explanation for the nonlinear response is that parasitized cells contain membrane pores whose conductivity is dependent upon the extracellular ion concentration. Our results indicate that the dielectrophoretic discrimination and separation of parasitized erythrocytes from blood should be feasible.

2. Materials and methods

2.1. Blood cells

Human blood (group 'O') was collected from healthy donors into sterile bags containing citrate phosphate dextrose as anticoagulant. Aliquots of 50 ml were transferred aseptically into screw-capped bottles, stored at 4°C, and used within three weeks of collection. Prior to use, an aliquot of 10 ml of the blood was transferred to a sterile screw-capped centrifuge tube and centrifuged ($800 \times g$, 10 min) to remove the plasma and buffy coat. The packed red

cell fraction was then twice washed in phosphate-buffered saline (pH 7.2) and cells were finally suspended at 50% hematocrit in RPMI 1640 medium containing 10% human serum as a stock for parasite cultivation.

2.2. Serum

Blood (type A, B, O or AB) was collected from healthy donors into sterile bags lacking anticoagulant. After clotting completely overnight at 4°C, the serum was separated by centrifugation ($800 \times g$, 20 min) and transferred to a sterile bag using a closed system procedure. Serum was inactivated for 30 min at 56°C and stored in sterile tubes at -20°C in aliquots of 10–20 ml.

2.3. Plasmodium falciparum cultures

Chloroquine-resistant strain T9/94 [35], a gift from Dr. P. Tan-Ariya of the Microbiology Department, Faculty of Science, Mahidol University, Bangkok, was grown in continuous culture using a complete RPMI 1640 medium containing 1 mM L-glutamine, 0.18% (w/v) $NaHCO_3$ and 10% human serum (pH 7.4). Cultures were maintained in 4-ml aliquots in 60 mm Petri plates in a candle jar (80% N_2 + 13% O_2 + 7% CO_2) at 37°C using the methods of Trager and Jensen [36]. The culture medium was changed every 24 h. Parasitemia was determined every 48–96 h by counting Giemsa-stained thin smears.

When parasitemia reached 6–8%, the Petri plates were pooled and the cells were recovered by centrifugation ($500 \times g$, 10 min), washed once in PBS (pH 7.2), and resuspended in complete medium at 50% hematocrit. Enough of this suspension was mixed with the fresh erythrocyte stock to yield a parasitemia of 0.5–1%. This suspension was then diluted with complete medium to yield a hematocrit of 6–8% and the culture was split between new Petri plates. In this way, the line was carried without parasitemia ever exceeding 10%.

To provide parasitized cells for dielectric measurements, ring stage synchronization of cultures was first accomplished using a slight modification of the method of Lambros and Vanderberg [37]. Briefly, a culture at 5–8% parasitemia was harvested by centrifugation ($500 \times g$, 10 min). The cells were then resuspended in 5% (w/v) D-sorbitol (Sigma Chemical Co.), incubated at 37°C for 20 min, centrifuged ($500 \times g$, 10 min), and washed twice in PBS (pH 7.2) to remove the sorbitol. The resulting parasitized cells, now synchronized at ring stage, were then diluted with complete medium to 2% hematocrit and cultured with a change of medium every 12 h. After 5–6 days, parasitemia reached 30–40% as determined from Giemsa-stained thin smears. These procedures together with the physical properties and morphology of parasitized erythrocytes are described and illustrated in detail in reference [38]. The culture was then harvested to provide a sample for dielectric measurements in which a large proportion of the cells were parasitized.

2.4. Electrorotation (ROT) and conventional dielectrophoretic (DEP) measurements

For ROT measurements, erythrocyte cultures exhibiting 30–40% parasitemia were diluted with 24 parts of medium a 8.5% (w/v) sucrose + 0.3% (w/v) dextrose solution to yield a suspension containing approximately $5 \cdot 10^5$ cells/ml at a conductivity of 56 mS/m. Approximately 100 μl of this suspension was sealed into a 1-mm deep chamber consisting of an 'O'-ring waxed to the surface of a microscope slide supporting a polynomial electrode [39]. A coverslip was pressed in place to seal the top. Four sine signals in phase quadrature were applied to the polynomial electrode to provide a rotating electrical field using the principles described earlier [29]. Cell rotation induced by the applied rotating field was measured by stopwatch with the aid of video microscopy as a function of the applied rotating field frequency over the range 1 kHz to 100 MHz. A large video monitor coupled to $\times 400$ optics made it possible to identify the parasitized and normal cells without recourse to staining or other identification techniques. Only those cells close to the center of the electrode geometry (where the electric field is uniform [40]) were measured to ensure that negligible lateral motions occurred so that the cells did not experience significant changes in their local electrical field strength in the course of the ROT determinations. Approximately 20 parasitized cells and 20 normal cells were timed at 4 points per decade of the frequency range studied. The diameter of each cell,

calibrated against a stage micrometer, was determined from its image on the TV monitor.

DEP crossover frequency measurements were conducted with the same polynomial electrode geometry and chamber but for these studies only two (out of phase) signals were used to generate an inhomogeneous, standing electrical field distribution between the electrode pole tips. Cells that were about 10 diameters away from the electrode edges (where the field becomes very inhomogeneous [40]) were measured. The electrical field was applied at a trial frequency (typically 20 kHz) and as soon as it was determined whether the resulting DEP force was inducing cell motion towards or away from the closest electrode edge (typically observation was for only about 1 s), the field was removed. The frequency was increased or decreased according to whether the cell moved away from the electrode edge (negative DEP) or towards it (positive DEP) until the DEP crossover-frequency, the frequency at which the DEP force was zero, was determined. Signals of 3–5 V (peak–peak) were normally employed on the 400-μm (pole tip to pole tip) electrodes, with voltages up to 8 volts (peak–peak) occasionally being applied for measurements very close to the crossover frequency where DEP-induced motion was slow. Measurements were taken for cell suspending medium conductivities in the range 1 to 75 mS/m. Suspension conductivities were adjusted to target values with KCl and measured using a digital conductivity meter (Cole-Palmer Model 1481-61). For each suspension conductivity a fresh sample of the parasite culture was taken and diluted and at least ten cells were measured. Finally, the repeatability of the experiment was verified by performing the measurements on at least three occasions on different culture passages.

2.5. Analysis of ROT data

In our experiments erythrocytes rested with their discoid faces parallel to the chamber bottom and, for the purpose of analyzing electrorotation experiments, these can be approximated as single shelled oblate spheroids of radially-symmetric radius r rotating about a minor axis (half-length c) lying normal to the chamber bottom. A detailed analysis of electrorotation for this case has been provided by Kakutani et al. [41]. Here we use that model to analyze the ROT data and adapt it for analysis of DEP crossover measurements. The complex polarizability at angular frequency ω along the major axes of the oblate spheroid can be written [41]

$$\mu_\alpha(\omega) = V_c \; {}_0 \frac{\tilde{\varepsilon}_p^* - \tilde{\varepsilon}_s^*}{(\tilde{\varepsilon}_p^* - \tilde{\varepsilon}_s^*) A_{0p} + \tilde{\varepsilon}_s^*} \tag{1}$$

where $\tilde{\varepsilon}_s^*$ and $\tilde{\varepsilon}_p^*$ are the effective complex permittivities of the suspending medium and of the ellipsoidal cell in the x–y plane, respectively, and V_c is a volume term. The depolarization parameter A_{0p}, from just outside the membrane to infinity, is a constant for a given cell geometry [41]

$$A_{0p} = \frac{\left[p_0^2/(p_0^2-1)^{\frac{1}{2}} \right] \arctan(p_0^2-1)^{\frac{1}{2}} - 1}{2(p_0^2-1)} \text{ where}$$

$$p_0 = \frac{r}{c} \tag{2}$$

The complex permittivity of the particle in Eq. (1) is [41]

$$\tilde{\varepsilon}_p^* = \tilde{\varepsilon}_M^* \frac{\tilde{\varepsilon}_M^* + (\tilde{\varepsilon}_I^* - \tilde{\varepsilon}_M^*)\left[A_{1p} + \upsilon(1 - A_{0p}) \right]}{\tilde{\varepsilon}_M^* + (\tilde{\varepsilon}_I^* - \tilde{\varepsilon}_M^*)(A_{1p} - \upsilon A_{0p})} \tag{3}$$

where $\tilde{\varepsilon}_M^*$ and $\tilde{\varepsilon}_I^*$ are the complex permittivities of the cell membrane and interior, respectively, A_{1p} is the depolarization factor integrated from just inside the membrane to infinity, $\upsilon = r^2 c/[(r+d)^2(c+d)]$ is the volume ratio of the cell exterior to interior and d is the membrane thickness. In the case of erythrocytes, d is approximately three orders of magnitude less that r and c, and we may make the approximation that $A_{1p} = A_{0p}$ so that Eq. (3) reduces to

$$\tilde{\varepsilon}_p^* = \tilde{\varepsilon}_M^* \left\{ \frac{\dfrac{1}{\upsilon} + \dfrac{a(\tilde{\varepsilon}_I^* - \tilde{\varepsilon}_M^*)}{(\tilde{\varepsilon}_I^* + a\tilde{\varepsilon}_M^*)}}{\dfrac{1}{\upsilon} - \dfrac{a(\tilde{\varepsilon}_I^* - \tilde{\varepsilon}_M^*)}{(\tilde{\varepsilon}_I^* + a\tilde{\varepsilon}_M^*)}} \right\}, \tag{4}$$

where $a = (1 - A_{0p})/A_{0p}$. Eq. (1) and Eq. (4) differ from the case of a single shelled spherical model [42,43] only by the introduction of geometrical constants so that a minor adaption of the numerical optimization approach applied by us previously [29,30] for analyzing ROT data of spherical cells could be used to derive values for the membrane and interior dielectric parameters of erythrocytes through

a MATLAB (The Math Workshop) implementation. In this analysis it was assumed that $p_0 = r/c = 2$ for the erythrocytes (whence $A_{0p} = 0.236$ and $a = 3.24$). The ROT rate is given by $R(\omega) = -h \cdot \mathrm{Im}[\mu_\alpha(\omega)]$ where the parameter h took into account the applied electrical field strength and rotational drag as described previously [30]).

2.6. Analysis of DEP data

To analyze the DEP crossover frequency data, we note that the time-averaged DEP force is zero when the real part of its polarization is zero. Setting $Re[\mu_\alpha(\omega)] = 0$ in Eq. (1) and rearranging, we obtain the crossover frequency

$$f_{co} = \frac{1}{2\pi}\left\{\frac{-\left[(1-A_{0p})\sigma_s + A_{0p}\sigma_p\right](\sigma_s - \sigma_p)}{\left[(1-A_{0p})\ _s + A_{0p}\ _p\right](\ _s - \ _p)}\right\}^{\frac{1}{2}}, \quad (5)$$

where and σ are the (real) permittivity and conductivity of the particle and its suspending medium (as denoted by the subscripts p or s), respectively. For a sphere $c = r$ and A_{0p} assumes the value $1/3$ so that this expression reduces to the simpler form used by us previously [44] and also corresponds to that for the cutoff frequency for the dielectrophoretic levitation of spheres [45]. Because our DEP crossover experiments were confined to frequencies well below the Maxwell–Wagner dispersion frequency and because the cell interior can be assumed to be much more conductive than the membrane we can also assume that $^*_M \ll \ ^*_I$. Under these conditions and using a first order expansion for $1/\nu$, Eq. (4) simplifies to

$$^*_p = \frac{rc}{(2c+r)da} \cdot \ ^*_m$$

whence

$$_p = \frac{br}{a} \cdot C_{\mathrm{spmem}} \text{ and } \sigma_p = \frac{br}{a} \cdot G_{\mathrm{spmem}}, \quad (6)$$

where $b = \dfrac{c}{(2c+r)}$, and C_{spmem} and G_{spmem} are the specific (per unit area) capacitance and conductance of the membrane, respectively. Substitution into Eq. (5) finally yields the expression for the crossover frequency of the oblate spherical cell in terms of its membrane electrical characteristics:

$$r \cdot f_{co} = \frac{A_{0p}}{2\pi bC_{\mathrm{spmem}}}\left\{\left(\sigma_s - \frac{br}{A_{0p}}G_{\mathrm{spmem}}\right) \times \left[\left(\frac{1-A_{0p}}{A_{0p}}\right)\sigma_s + \frac{br}{A_{0p}}G_{\mathrm{spmem}}\right]\right\}^{\frac{1}{2}} \quad (7)$$

In the case of a sphere, $A_{0p} = b = 1/3$ and the expression reduces to that used previously to analyze the DEP crossover frequency of spherical cells [44]. For other cell geometries Eq. (7) differs from the expression for the spherical case only by the introduction of geometrical constants. If C_{spmem}, S_{spmem} and r/c are independent of the suspending medium conductivity σ_s then a plot of $f_{co} \cdot r$ versus σ_s will have a slope

$$\frac{\left[A_{0p}(1-A_{0p})\right]^{\frac{1}{2}}}{2\pi bC_{\mathrm{spmem}}}$$

when $\sigma_s \gg \sigma_{\mathrm{mem}}$ and an intercept derived by extrapolating the linear region of the plot back to the σ_s axis

$$\frac{brG_{\mathrm{spmem}}(1-2A_{op})}{2A_{op}(1-A_{op})}.$$

Alternatively an optimization algorithm can be used to fit Eq. (7) directly to the crossover frequency data. Thus the specific cell membrane capacitance and conductance can be readily estimated from DEP crossover characteristics of oblate cells providing the cell geometry is known. Finally, we note that while the extrapolated intercept on the σ_s axis will always assume a positive value if the cell dielectric properties and geometry remain constant, non-linearity can occur and a negative intercept on the σ_s axis will no longer be forbidden in more complex cases where C_{spmem}, σ_{mem} or r/c depend on σ_s.

3. Results

3.1. Electrorotation (ROT) measurements

Typical ROT spectra are shown in Fig. 1 for normal erythrocytes and for erythrocytes containing

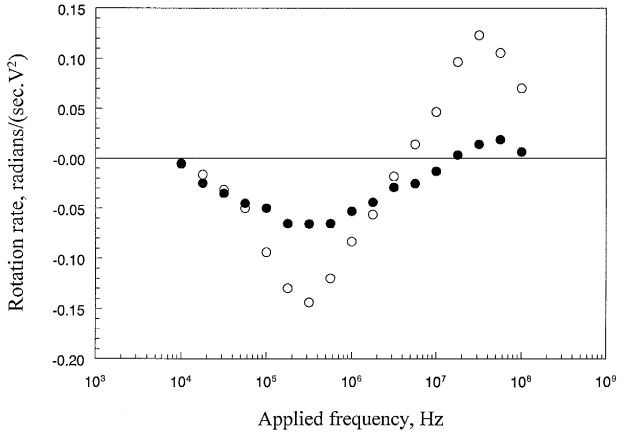

Fig. 1. Electrorotation spectra for single erythrocytes. While the spectrum shown for the normal erythrocyte (○) is typical and was stable for at least 40 min, spectra for cells infected with the malarial parasite *Plasmodium falciparum* exhibited great variability and changed over the 10–20-min period needed to measure a spectrum. The example spectrum for a parasitized cell (●) shows a slight shift in frequency of the antifield (negative-going) rotation peak but a serious depression of the cofield peak compared with the spectra for normal cells. Note that the ordinate units have not been corrected for the field in the locality of each cell but instead reflect the voltage applied to the quadripolar polynomial electrodes.

parasites. Spectra for different uninfected cells were found to be almost identical, indicating a reasonably high degree of homogeneity within the normal erythrocyte population. Furthermore, by measuring the same uninfected cells several times it was possible to show that their dielectric properties remained essentially constant over a period of 45 min or more under our measurement conditions. The spectral shape for uninfected cells was similar to that observed previously for erythrocytes [32], with cell rotation occurring counter to the sense of the applied rotating field (antifield rotation) below 5 MHz and in the same sense as the field (cofield rotation) above that frequency at a suspension conductivity of 56 mS/m. Peak rotation rates for the normal cells occurred at 260 kHz (anti-field peak where the cell rotation is contrary to the field direction) and approximately 40 MHz (co-field peak where the cell rotates in the same sense as the field).

The characteristic shape of the ROT spectra observed for the normal cells is well described by the single shell dielectric model that regards the cell as a homogeneously conductive cytoplasm surrounded by a single, thin, dielectric membrane [41–43]. We therefore applied the same non-linear parameter optimization methods that we reported earlier [29] to fit the single-shell oblate-spheroid dielectric model to the ROT spectrum of Fig. 1 for normal erythrocytes. This analysis yielded values of 12 ± 1.2 mF/m^2 for the plasma membrane specific capacitance (in good agreement with the value reported by others [46,47]), 0.52 ± 0.05 S/m for the cytoplasmic conductivity, and 57 ± 5.4 for the internal relative permittivity of the uninfected cells. Our recent analysis of the accuracy of dielectric data obtained from such ROT measurements shows that under these circumstances the membrane conductivity cannot be accurately determined (and no value will be given here, therefore) while other parameters are accurate to within the given error limits at a 90% confidence level [30].

In contrast to the relatively high degree of homogeneity observed for uninfected erythrocytes, those containing parasites exhibited a high degree of variability. All showed deviations from the ROT spectra characteristic of healthy cells and, in general, the peak counter-field rotation rate, which occurred at about 260 kHz for uninfected cells, was shifted in frequency by around 50 kHz and its height was only 30% to 50% of that seen for normal cells. Most dramatically, the cofield rotation peak was initially only 10% to 30% of that characteristic of normal cells and diminished in magnitude and frequency with time over a period of 10–20 min. In extreme cases, it almost disappeared. It was difficult to make ROT spectral measurements on the parasitized cells because of these changes with time.

It is well-established [29,41–43] that the antifield and cofield rotation peak heights and positions are determined by the electrical properties of the plasma membrane and cell interior, respectively. The antifield peak characteristics depend on the plasma membrane capacitance (which reflects the membrane thickness, composition and morphological complexity [29]) and the membrane conductance (which reflects the transposition of charge carriers across the membrane through membrane channels, pores and defects under the influence of the applied a.c. electrical field). The magnitude and characteristic frequency of the higher frequency cofield peak, on the other hand, are indicative of the effective dielectric permittivity of the cell interior (which reflects the combined

properties of the cytoplasmic water and of intracellular barriers to charge movement) and of the effective cell interior conductivity (which is dominated by the electrical mobility of ionic species). The changes in the cofield peak observed with time in our ROT experiments on parasitized erythrocytes were consistent with a drop in cytoplasmic conductivity most likely resulting from net ion outflux from the cytoplasm. This suggested to us that parasitized cells possessed a much higher membrane conductivity than normal erythrocytes.

Unfortunately, a limitation of the ROT method is that only four model parameters may be accurately determined from spectra consisting of two peaks when the local electrical field strength and the frictional resistance to rotation are unknown [30]. This presents no difficulty in the interpretation of the ROT spectra of cells such as the normal erythrocytes that have plasma membranes of low conductivity (see for example Ref. [29]), but in the present case it limited the accuracy with the membrane parameters of the infected cells could be deduced. For this reason, as well as the instability of the ROT data of parasitized cells during measurement, the alternative electrokinetic method of measuring cell DEP crossover frequencies as a function of the suspending medium conductivity was used to further characterize the differences between uninfected and infected erythrocytes.

3.2. Dielectrophoretic (DEP) measurements

Unlike ROT measurements for which parameters are derived on a single-cell basis, several cells can be investigated and a plot derived from which dielectric data can be deduced by this DEP method. Nevertheless, cells can be individually selected so that specific subpopulations (in our case, parasitized cells) in a mixture can still be targeted for measurement. The method also offers the advantage that measurements on each cell can be completed within about 1 min so that the extent of net ion outflux from the cytoplasm to the supporting medium is limited compared to ROT spectral measurements. Finally, the technique works well for determining both the membrane capacitance and conductance even when the membrane conductance is high.

Fig. 2 shows the DEP crossover frequency times the cell radius plotted for normal and parasitized cells as a function of the suspending medium conductivity. While uninfected cells exhibited a linear dependency and a small mean coefficient of variance of 0.05, parasitized cells showed a non linear dependency and, depending upon the medium conductivity, a coefficient of variance up to 0.5 indicative of hetero-

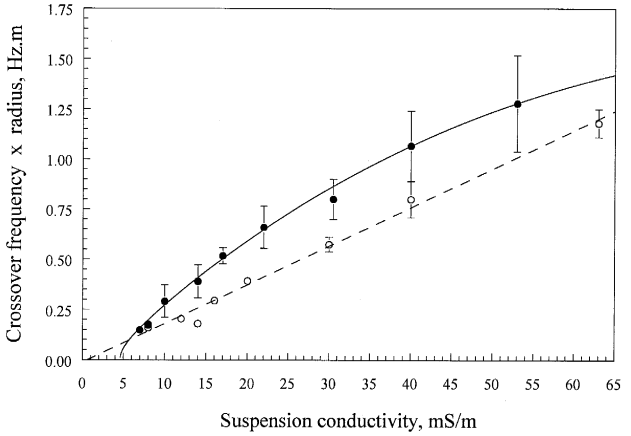

Fig. 2. Dielectrophoretic crossover frequency characteristics of normal human erythrocytes (○) and of human erythrocytes infected with the malarial parasite *Plasmodium falciparum* (●) as a function of the cell suspension conductivity. Points reflect the means and error bars the standard deviations; the number of samples, n, was $5 \leq n \leq 12$ in each case. Best fits of Eq. (7), as discussed in detail in the text, are shown.

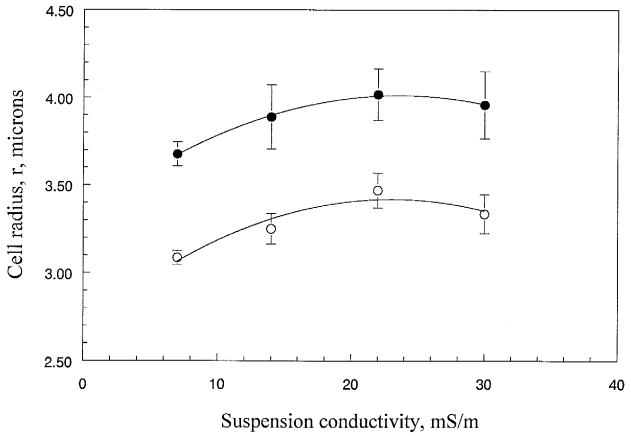

Fig. 3. Dependence of the radius of normal (○) and parasitized (●) human erythrocytes on the cell suspension conductivity. Solutions were maintained at physiological tonicity with 8.5% sucrose + 0.3% dextrose. Points reflect the means and error bars the standard deviations; the number of samples, n, was $5 \leq n \leq 12$ in each case. The empirical fits shown are quadratic.

geneity. Such heterogeneity was not unexpected, however, since the parasite cultures were asynchronous with respect to parasite phase when they were examined.

As shown in Fig. 3, the radius of parasitized cells was found to be significantly higher than for normal cells and the radius of both normal and parasitized cells was a weak function of the suspending medium conductivity, increasing by about 10% as the medium conductivity was increased from 7 to 22 mS/m and decreasing slightly thereafter. This radius response was almost certainly not osmotic in origin since initially it was counter to that expected for increasing suspending medium tonicity and, in any case, the tonicity variation due to adjustment of the suspension conductivity was only 1% at most.

4. Discussion

4.1. Cell electrorotation

Normal erythrocytes behaved in ROT experiments (see Fig. 1) as other mammalian cell types for which we and others have reported data [29–32]. Their ROT spectrum can be readily understood in terms of the single-shell dielectric model in which the cell is approximated as a homogeneous, conductive, aqueous cytoplasm surrounded by a thin, dielectric membrane [41–43]. In earlier studies we demonstrated that the ROT method is useful for sensitively detecting changes in the dielectric properties of cells such as those accompanying induced differentiation of Friend murine erythroleukemia [29]. Similar analysis techniques adapted to the oblate spheroid geometry of the cells were applied here to study the uninfected erythrocytes and dielectric properties of single cells were obtained to an accuracy of 10% with a 90% confidence level [30]. The derived mean specific capacitance value of 10 ± 1.0 mF/m^2 is in agreement with previous determinations on bulk erythrocyte suspensions [46,47] and is consistent with the value expected for a cell with a smooth plasma membrane [29].

ROT spectra of parasitized erythrocytes were significantly different from those of uninfected cells and exhibited great variability from one cell to another. Because the spectra of parasitized cells altered during the course of measurement, parameters derived from quantitative analyses of the data were suspect. Nevertheless, simulations using the single shell dielectric model allowed us to deduce that the observed spectral shapes could have resulted from a large (> 1500 S/m^2) cell membrane conductance in infected cells coupled with a steadily falling cytoplasmic conductivity. In view of the earlier bulk cell suspension dielectric studies by Aceti et al. [24] and the known erythrocyte membrane permeability increases towards a variety of molecules following malaria infection [2,3,20,21], such a finding is not surprising. The large conductance and associated ion loss rate overwhelmed the ROT technique, however this in itself is of interest because it suggests that ROT might be able to probe more subtle parasitization events such as initial merozoite entry into erythrocytes and early parasite-induced membrane alterations. Since ROT is ideal for the non-invasive study of viable cells, such events might be resolvable in real time.

4.2. Dielectrophoretic crossover of normal cells

To better understand the dielectric changes in erythrocytes accompanying parasitization events, we resorted to using the DEP crossover method. Because only one frequency point was required for each cell for this technique as compared to an entire frequency spectrum comprising 20 points for the ROT method, the amount of time spent on each cell in a DEP crossover measurement was about 1 min compared to 20 min for a ROT measurement. Cells could therefore be measured quickly following suspension in low conductivity medium during crossover frequency measurements and cytoplasmic ion loss was very much less of a problem than in the ROT case. Unfortunately, this speed advantage of the DEP method came at the expense of not being able to derive dielectric parameters for each individual cell, however.

Fig. 2 shows that the product of the DEP crossover frequency and cell radius $f_c \cdot r$ of uninfected erythrocytes depended linearly on the suspending medium conductivity σ_s in a fashion that was consistent with a single shell dielectric model having constant membrane specific capacitance (C_{spmem}) and conductance (G_{spmem}) values and a fit of Eq. (7) to the data with $r/c = 2$ yielded values of 11.8 mF/m^2 and 271

S/m^2, respectively, for these parameters. It is important not to confuse membrane conductance parameter G_{spmem} derived here with the trans-membrane conductance parameter G_{tmem} measured by electrophysiological techniques such as patch-clamping. G_{spmem} reflects the contributions of all processes that influence the effective medium conductivity in the vicinity of the cell. Thus in addition to the well-known electrophysiological term G_{tmem}, which describes the conductivity *through* the cell membrane, an additional conductivity contribution K_{mem} that lies tangential to the membrane surface and which represents conductivity *around* the cell also contributes to [48] G_{spmem} so that

$$G_{spmem} = G_{tmem} + \left(\frac{2K_{mem}}{r^2} \right). \quad (8)$$

It follows that the trans-membrane conductance G_{tmem} cannot be derived unambiguously from the dielectrophoresis data presented here. Furthermore, when the cell diameter becomes small, as is the case for erythrocytes, the contribution from K_{mem} may become much larger than G_{tmem}. Assuming a value of 1 mS/m for G_{tmem}, as typically observed for mammalian cells by patch-clamping techniques, a value of $K_{mem} = 5.4 \cdot 10^{-10}$ S is obtained. This tangential conductivity contribution arises from the high concentration of counterions in the charge double layer associated with the cell surface charge [49] and from the enhanced mobility of charge carriers such as protons associated with the glycocalyx [50,51]. Although this conductivity value is very small, the very small size of erythrocytes works through the square law dependency on cell radius in Eq. (8) to allow its contribution to swamp that of G_{tmem}.

4.3. Dielectrophoretic crossover of parasitized cells

In striking contrast to normal erythrocytes, the non-linear crossover frequency response of parasitized cells did not fit a simple model. Instead, the data shows that the membrane capacitance, conductance or cell geometry for these cells must have altered as a function of the suspending medium conductivity, and we shall now consider these possibilities.

4.3.1. Variable cell specific conductance, G_{spmem}

Since we suspected from our ROT observations and simulations that the membrane conductance of the parasitized cells was significantly altered compared with healthy erythrocytes, we first investigated whether variations in G_{spmem} could account for the observed crossover frequency characteristics. Linear and quadratic dependencies of membrane conductance as a function of suspension conductivity did not fit the experimental data, however a good fit over the suspension conductivity range examined was obtained when the membrane specific conductance varied according to

$$r \cdot G_{spmem} = \sigma_0 + \sigma_s \left(1 - \exp\left(\frac{-\sigma_s}{\sigma_k} \right) \right) \quad (9)$$

This empirical relationship engenders the essential characteristics that the membrane conductance of the parasitized cells was small ($r\sigma_0$) when the suspending medium conductivity (σ_s) was small but rose as σ_s increased. The solid line through the data points for parasitized cells in Fig. 2 shows a fit of Eq. (9) with σ_0 and σ_k having values of 4.25 mS/m and 58 mS/m, respectively. The membrane specific capacitance is then derived as 9 mF/m^2 and the membrane specific conductance, G_{spmem}, at a suspension medium conductivity of $\sigma_s = 5$ mS/m is found to be 1130 S/m^2, almost 4-times that found for normal erythrocytes, and rises with increasing suspension conductivity. The variation of membrane conductance that provides the fit shown in Fig. 2 is illustrated as the solid curve in Fig. 4 (left-hand ordinate), where it can be seen that an increase of a factor of ten occurs over the range of suspension conductivities studied here. While Eq. (9) suggests that the membrane conductance increases indefinitely with increasing suspension conductivity, it seems more likely that it would saturate at some upper limit. Therefore we consider that Eq. (9) is probably only useful for the suspension conductivity range studied here.

It follows that the crossover frequency data observed here for parasitized cells can be explained in terms of changes in the membrane specific conductance with suspension conductivity. While it is not clear whether such increased conductance would have arisen from a change in transmembrane specific con-

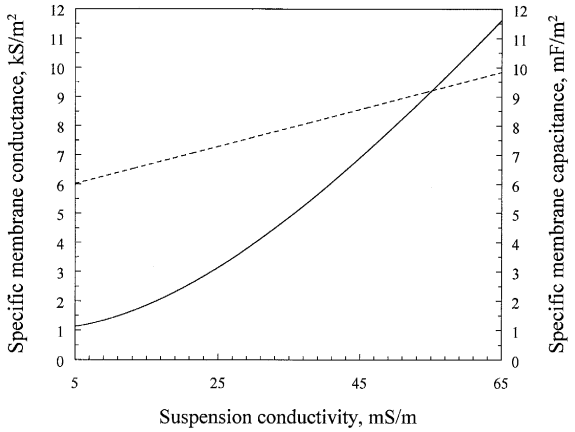

Fig. 4. Possible interpretations of the non-linearities of the dielectrophoretic crossover characteristics of parasitized cells observed in Fig. 2. The experimental data can be accurately modelled if the specific membrane conductance (left-hand ordinate and solid curve) *or* the specific membrane capacitance (right-hand ordinate and dashed line) of the parasitized cells is allowed to vary with the cell suspension conductivity as shown.

ductance G_{tmem} or in tangential membrane conductivity K_{mem}, the apparent rapid ion outflux from the cytoplasm during ROT experiments and evidence that the erythrocyte membrane becomes highly permeable to a variety of solutes during parasite development [20,21,52] together suggest that the transmembrane component would most likely be involved. If this is the case then the transmembrane conductance of the parasitized cells G_{tmem} is more than 3 orders of magnitude larger than for a typical mammalian cell and dominates G_{spmem}, indicating that the permeability of the membrane of late-stage parasitized cells to ions under our experimental conditions is extremely large.

4.3.2. Variable cell specific capacitance, C_{spmem}

A possible alternative explanation for the crossover frequency data for parasitized cells is that the specific membrane conductance remains fixed but its specific capacitance alters with suspension conductivity. In this case, the required variation in C_{spmem}, follows a simpler linear relationship

$$C_{spmem} = C_{spmem0} + k_c \cdot \sigma_s \quad (10)$$

The corresponding relationship between C_{spmem} and the suspension conductivity is shown by the broken line in Fig. 4 (right hand ordinate) where C_{spmem0} and k_c have the values 5.7 mF/m^2 and 0.063 $(mF/m^2)/(S/m)$, respectively. From this it can be seen that the specific membrane capacitance would have to increase from 6 mF/m^2 at a suspension conductivity of 5 mS/m to 9.9 mF/m^2 at the highest value for which measurements were made to fit the crossover frequency data. The membrane specific conductance would remain constant at 1000 mS/m^2.

Variations in C_{spmem} could be brought about by changes in membrane thickness and dielectric composition. However, the extent of such changes for typical biological membranes are limited to approximately 15%, too small to account for the required variation here, and in any case it is hard to see how these membrane parameters could have responded immediately to changes in the cell suspension conductivity. Larger changes in cell membrane specific capacitance can be induced by alterations in membrane surface morphology [29] comprising ruffles, folds, microvilli, blebs and other features that contribute to a larger membrane area than is needed to cover a smooth cell. Such increased membrane area results in a correspondingly higher measured specific capacitance value and changes in membrane capacitance by up to 40% have been attributed to such alterations induced by chemical or physical agents [29,44]. A variation of some 10% in the radius of parasitized cells was observed here as the suspension conductivity was increased (Fig. 3). Although this might have been paralleled by changes in membrane conformation, such a 10% change radius is not only too small to provide for the almost twofold change needed in membrane capacitance but also too complex in terms of its dependence on suspension conductivity to provide a linear dependence of C_{spmem}. We also note that an identical radius response occurred in uninfected erythrocytes which exhibited a linear crossover frequency characteristic. Finally, the value of 6 mF/m^2 required at small suspension conductivities seems anomalously low for the erythrocyte plasma membrane capacitance since it is generally accepted that biological membranes have capacitances above 8 mF/m^2. These factors lead us to conclude that changes in membrane specific capacitance did not account for the observed non-linearities in the DEP crossover behavior even though the re-

quired dependency with suspension conductivity is simple in form.

4.3.3. Variable cell shape

Throughout the analysis it has been assumed that the erythrocytes can be described by a single shell, oblate spherical dielectric model with a constant minor to major axis ratio r/c of 2. It is certainly conceivable that small alterations in r/c could have occurred as a function of the medium conductivity. To test whether such changes could have accounted for the non-linearities in the DEP crossover characteristics of parasitized cells, we investigated the extent of r/c variations that would be needed to account for the experimental data. Fig. 5 shows our experimental DEP crossover data for the parasitized cells plotted with a family of simulated crossover characteristics for the range $r/c = 1.25$ to $r/c = 6$ for the conditions $G_{\text{spmem}} = 1200$ mS/m and $C_{\text{spmem}} = 10$ mF/m^2. It can be deduced from the manner in which the experimental data overlays the simulated characteristic curves that the factor r/c would have had to vary from 5.5 to 1.3 over the suspension conductivity range 5 mS/m to 55 mS/m in order to account for the experimental findings. No changes in cell appearance were observed over this range except for the 10% variation in cell diameter already discussed (Fig. 3). Since it is implausible that the cell thickness could have changed by a factor of more than 4 without any significant alteration in cell diameter or appearance, this mechanism can be ruled out as an explanation for the non-linearities of the DEP crossover characteristics.

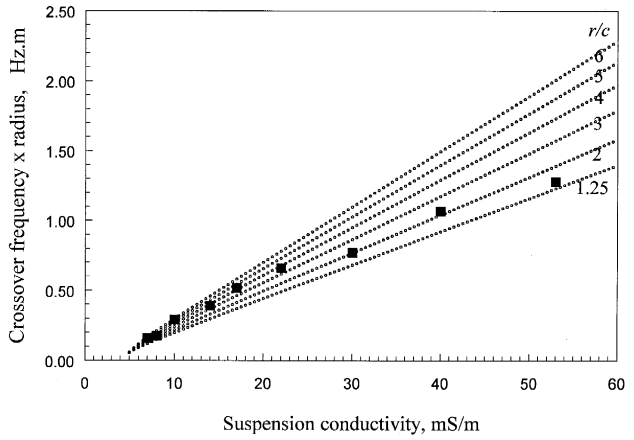

Fig. 5. Non-linearity of the dielectrophoretic crossover data for parasitized cells could also be accounted for by variations in the cell geometry. Each dotted characteristic represents a simulated cell response for a different major to minor axis ratio r/c of the erythrocytes. However, inspection of the disposition of the experimental data (■) with respect to the simulated characteristic lines reveals that the axis ratio would need to vary from 5.5 to 1.3 over the suspension conductivity range studied for this mechanism to account for the non-linearity observed.

Thus while the observed non-linear crossover frequency characteristics of parasitized cells could in principle be explained by dependencies of specific membrane conductance, capacitance or shape, the most likely origin is a variation in the membrane conductance. The very high membrane conductance we project at 56 mS/m^2 almost certainly arises from the transmembrane component of conductance since ions were rapidly depleted from the cytoplasm during ROT measurements at this conductivity value.

We therefore conclude that infected cells had a very high transmembrane conductance (as high as $\approx 10^3$ S/m^2) that depended on the suspending medium characteristics. This dependency suggests that the conductivity of the parasitized cell membranes probably does not arise from indiscriminate perforations or disruptions of the plasma membrane but instead is mediated by modifiable pores. As already indicated it is well established that parasites strongly modify the transport properties of their host cells for a variety of both charged and neutral molecular species [20,21,52]. Kutner et al. [20] have shown that these permeation pathways begin to appear about 6 h after infection of the erythrocyte, that they exhibit selectivity towards a range of solutes, that the enthalpy of activation for each solute is not a function of the total permeability of the membrane, and that parasite protein synthesis is a prerequisite for the permeation to occur. All of these observations are consistent with the hypothesis that the permeation arises from protein channels that are synthesized by the parasite, probably for the purpose of controlling solute exchange by the host cell.

The mechanism by which membrane pores in the infected cells could be affected by changes in the suspending medium conductivity is unclear, however we note that the extracellular conductivity was manipulated in our experiments by adjusting the concentration of KCl in the suspension. This manipulation would have altered not only the external ion comple-

ment and extent of the charge double layer at the membrane surface but also the ratio of cytoplasmic to extraerythrocytic ions and might have influenced the erythrocyte transmembrane potential. The superlinear–linear form of the membrane conductance found for the infected cells (Eq. (9)) suggests that the ability of ions to cross the membrane barrier was influenced by one of these parameters. It is well known that membrane conformation as well as membrane channel activities tend to be strongly ion dependent and cellular metabolic activities may also have been modified. Kirk et al. [52] have shown that the transport of a wide range of solutes into erythrocytes infected with *P. falciparum* including monovalent ions, neutral amino acids, and sugars was associated with a single, anion-selective pathway that had some similarities to chloride channels in other cell types. Our observations seem to be compatible with such an ion-channel interpretation. If the increased cell membrane conductance observed by us in parasitized cells can indeed be attributed to pores, our observations would represent the first time ion-channel activities have been directly observed by dielectrophoresis.

Finally, we have demonstrated previously that differences in the dielectric properties of different cell types can be exploited for the purpose of cell separations [31–34]. The data presented here clearly show that dielectric differences between malarially-parasitized erythrocytes and their healthy counterparts are larger than those previously exploited for separating human breast cancer cells [32], leukemia cells [31] and hemopoietic stem cells [34] from whole blood. We therefore suggest that it should prove possible to separate parasitized cells from whole blood using dielectrophoresis. This may have important diagnostic and research implications. Finally, the differences in cell membrane conductivity in cells from our cultures of high parasitemia were so large as to make it difficult to measure cell dielectric properties by electrorotation. We therefore suggest that electrorotation may prove to be a useful tool for investigating parasite entry into erythrocytes and for studying the earliest stages of parasite growth with high sensitivity. Such measurements may lead to new insights into parasite development and to a better understanding of the membrane permeation process. In particular, ROT might permit investigations in real time of the effects of anti malarial agents on the permeation pathway.

Acknowledgements

This work was supported by and conducted at the Chulabhorn Research Institute, Bangkok, Thailand. The authors gratefully acknowledge the skilful cytological work of Piyajit Watcharasit, and the valuable help of Drs. Xiaobo Wang, Ying Huang and Mark Talary. We are also greatly indebted to John Tame for making the electrodes used in this study.

References

[1] Howard, R.J. (1982) Immunol. Rev. 61, 67–107.
[2] Cabantchik, Z.I. (1990) Blood Cells 16, 421–432.
[3] Elford, B.C., Cowan, G.M. and Ferguson, D.J.P. (1995) Biochem. J. 308, 361–374.
[4] Aikawa, M. and Miller, L.H. (1983) in Malaria and the Red Cell, pp. 45–63, Ciba Foundation Symposium 94, London.
[5] Atkinson, C.T. and Aikawa, M. (1990) Blood Cells 16, 351–368.
[6] Aikawa, M. (1988) Biol. Cell. 64, 173–181.
[7] Butler, K.W., Deslauriers, R. and Smith, I.C.P. (1984) Exp. Parasitol. 57, 178–184.
[8] Vial, H.J., Ancelin, M.-L., Philippot, J.R. and Thuet, M.J. (1990) Blood Cells 16, 531–555.
[9] Maguire, P.A., Prudhomme, J. and Sherman, I.W. (1991) Parasitology 102, 179–186.
[10] Hsiao, L.L., Howard, R.J., Aikawa, M. and Taraschi, T. (1991) Biochem. J. 274, 121–132.
[11] Dluzewski, A.R., Fryer, P.R., Griffiths, S., Wilson, R.J.M. and Gratzer, W.B. (1989) J. Cell Sci. 92, 691–699.
[12] Baruch, D., Glickstein, H. and Cabantchik, Z.I. (1991) Exp. Parasitol. 73, 440–450.
[13] Pattanapanyasat, K., Udomsangpetch, R. and Webster, H.K. (1993) Cytometry 14, 449–454.
[14] Howard, R.J., Reuter, G., Barnwell, J.W. and Schauer, R. (1986) Parasitology 92, 527–543.
[15] Howard, R.J., Seeley, D.C., Kao, V., Wember, M. and Schauer, R. (1986) Parasitology 92, 545–557.
[16] Sabolovic, D., Canque, B., Berbiguier, N. and Galey, L. (1991) Cell. Dev. Biol. 27A, 595–596.
[17] Paulitschke, M. and Nash, G.B. (1993) J. Lab. Clin. Med. 122, 581–589.
[18] Allred, D.R., Sterling, C.R. and Morse, P.D. (1983) Mol. Biochem. Parasitol. 7, 27–39.
[19] Degercy, A., Schrevel, J., Duportail, G., Laustriat G. and Kuhry, J.G. (1986) Biochem. Int. 12, 21–31.
[20] Kutner, S., Baruch, D., Ginsburg, H. and Cabantchik, Z.I. (1982) Biochim. Biophys. Acta 687, 113–117.
[21] Ginsburg, H., Kutner, S., Krugliak, M. and Cabantchik, Z.I. (1985) Mol. Biochem. Parasitol. 14, 313–322.
[22] Ginsburg, H. (1990) Comp. Biochem. Physiol. 95A, 31–39.
[23] Zanner, M.A., Galey, W.R., Scaletti, J.V., Brahm, J. and Vander Jagt, D.L. (1990) Mol. Biochem. Parasitol. 40, 269–278.

[24] Aceti, A., Bonincontro, A., Cametti, C., Celestino, D. and Leri, O. (1990) Trans. R. Soc. Trop. Med. Hyg. 84, 671–672.
[25] Arnold, W.M. and Zimmermann, U. (1982) Z. Naturforsch 37c, 908–915.
[26] Gascoyne, P.R.C., Noshari, J., Becker, F.F. and Pethig, R. (1994) IEEE Trans. Industry Applic. 30, 829–834.
[27] Huang, Y., Hölzel, R., Pethig, R. and Wang, X.B. (1992) Phys. Med. Biol. 37, 1499–1517.
[28] Fuhr, G., Arnold, W.M., Hagedorn, R., Müller, T., Benecke, W., Wagner, B. and Zimmermann, U. (1992) Biochim. Biophys. Acta 1108, 215–223.
[29] Wang, X.-B., Huang, Y., Gascoyne, P.R.C., Becker, F.F., Hölzel, R. and Pethig, R. (1994) Biochim. Biophys. Acta 1193, 330–344.
[30] Gascoyne, P.R.C., Wang, X.-B. and Becker, F.F. (1995) Bioelectrochem. Bioeng. 36, 115–125.
[31] Becker, F.F., Wang, X.-B., Huang, Y., Pethig, R., Vykoukal, J. and Gascoyne, P.R.C. (1994) J. Phys. D Appl. Phys. 27, 2659–2662.
[32] Becker, F.F., Wang, X.-B., Huang, Y., Pethig, R., Vykoukal, J. and Gascoyne, P.R.C. (1995) Proc. Natl. Acad. Sci. USA 92, 860–864.
[33] Markx, G.H., Talary, M.S. and Pethig, R. (1994) J. Biotechnol. 32, 29–37.
[34] Talary, M.S., Mills, K.I., Hoy, T., Burnett, A.K. and Pethig R. (1995) Med. Biol. Engin. Computing 33, 235–237.
[35] Thaihong, S. and Beale, G.H. (1985) Bull. WHO 617–619.
[36] Trager, W. and Jensen, J.B. (1976) Science 193, 673–674.
[37] Lambros, C. and Vanderberg, J.P. (1979) J. Parasitol. 65, 418.
[38] W. Peter and W.H.G. Richards (eds.) (1984) Handbook of Experimental Pharmacology Vol.68/I. Antimalarial Drugs I, Springer-Verlag, New York.
[39] Huang, Y. and Pethig, R. (1991) Meas. Sci. Technol. 2, 1142–1146.
[40] Hughes, M.P., Wang, X.-B., Becker, F.F., Gascoyne, P.R.C. and Pethig, R. (1994) J. Phys. D Appl. Phys. 27, 1564–1570.
[41] Kakutani, T., Shibatani, S. and Sugai, M. (1993) Bioelectrochem. Bioenerg. 31, 131–145.
[42] Irimijiri, A., Hanai, T. and Inouye, A. (1979) J. Theor. Biol. 78, 251–269.
[43] Marszalek, P., Zielinski, J.J., Fikus, M. and Tsong, T.Y. (1991) Biophys. J. 59, 982–987.
[44] Huang, Y., Wang, X.-B., Becker, F.F. and Gascoyne, P.R.C. (1996) Biochim. Biophys. Acta (in press).
[45] Jones, T.B. and Kallio, G.A. (1979) J. Electrostatics 6, 207–224.
[46] Fricke, H. (1925) J. Gen. Physiol. 9, 137–152.
[47] Schwan, H.P. (1983) Blut 46, 185–197.
[48] Hu, X., Arnold, W.M. and Zimmermann, U. (1990) Biochim. Biophys. Acta 1021, 191–200.
[49] Bedzyk, M.J., Bommarito, G.M., Caffrey, M. and Penner, T.L. (1990) Science 248, 52–56.
[50] Gutman, M., Nachliel, E. and Moshiach, S. (1989) Biochemistry 28, 2936–2940.
[51] Morgan, H., Taylor, D.M. and Oliveira, O.N. (1988) Chem. Phys. Lett. 150, 311–314.
[52] Kirk, K., Horner, H.A., Elford, B.C., Ellory, J.C. and Newbold, C.I. (1994) J. Biol. Chem. 269, 3339–3347.